


Activation of insulin-like growth factor 1 receptor participates downstream of GPR30 in estradiol-17 β -D-glucuronide-induced cholestasis in rats

Ismael R. Barosso¹ · Gisel S. Miszczuk¹ · Nadia Ciriaci¹ · Romina B. Andermatten¹ · Paula M. Maidagan¹ · Valeria Razori¹ · Diego R. Taborda¹ · Marcelo G. Roma¹ · Fernando A. Crocenzi¹ · Enrique J. Sánchez Pozzi¹ 

Received: 30 June 2017 / Accepted: 17 October 2017
© Springer-Verlag GmbH Germany 2017

Abstract Estradiol-17 β -D-glucuronide (E17G), through the activation of different signaling proteins, induces acute endocytic internalization of canalicular transporters in rat, including multidrug resistance-associated protein 2 (Abcc2) and bile salt export pump (Abcb11), generating cholestasis. Insulin-like growth factor 1 receptor (IGF-1R) is a membrane-bound tyrosine kinase receptor that can potentially interact with proteins activated by E17G. The aim of this study was to analyze the potential role of IGF-1R in the effects of E17G in isolated perfused rat liver (IPRL) and isolated rat hepatocyte couplets. In vitro, IGF-1R inhibition by tyrphostin AG1024 (TYR, 100 nM), or its knock-down with siRNA, strongly prevented E17G-induced impairment of Abcc2 and Abcb11 function and localization. The protection by TYR was not additive to that produced by wortmannin (PI3K inhibitor, 100 nM), and both protections share the same dependency on microtubule integrity, suggesting that IGF-1R shared the signaling pathway of PI3K/Akt. Further analysis of the activation of Akt and IGF-1R induced by E17G indicated a sequence of activation GPR30-IGF-1R-PI3K/Akt. In IPRL, an intraportal injection of E17G triggered endocytosis of Abcc2 and Abcb11, and this was accompanied by a sustained decrease in the bile flow and the biliary excretion of Abcc2 and Abcb11 substrates. TYR did not prevent the initial decay, but it greatly accelerated the

recovery to normality of these parameters and the reinsertion of transporters into the canalicular membrane. In conclusion, the activation of IGF-1R is a key factor in the alteration of canalicular transporter function and localization induced by E17G, and its activation follows that of GPR30 and precedes that of PI3K/Akt.

Keywords Abcb11 · Abcc2 · IGF-1 receptor · Cholestasis · ABC transporters

Abbreviations

Abcc2	Multidrug resistance-associated protein 2
Abcb11	Bile salt export pump
E17G	Estradiol 17 β -D-glucuronide
EGFR	Epidermal growth factor receptor
ER α	Estrogen receptor alpha
GPR30	G protein-coupled receptor 30
IGF	Insulin-like growth factor 1
PI3K	Phosphoinositide 3-kinase
Akt	Protein kinase B
CMFDA	5-Chloromethylfluorescein diacetate
GS-MF	Glutathione methylfluorescein
CGamf	Cholyl-glycylamido-fluorescein
DMSO	Dimethyl sulfoxide
IRHC	Isolated rat hepatocyte couplets
SCRH	Sandwich-cultured rat hepatocytes
cVA	Canalicular vacuolar accumulation
IPRL	Isolated perfused rat liver

Electronic supplementary material The online version of this article (doi:10.1007/s00204-017-2098-3) contains supplementary material, which is available to authorized users.

✉ Enrique J. Sánchez Pozzi
esanchez@unr.edu.ar

¹ Instituto de Fisiología Experimental (IFISE), Facultad de Ciencias Bioquímicas y Farmacéuticas (CONICET-U.N.R.), Suipacha 570, S2002LRL Rosario, Argentina

Introduction

Bile formation is a highly regulated physiological process. It depends on the coordinated action of a number of transporters in the sinusoidal and canalicular domains of

hepatocytes that mainly belong to the ABC superfamily of ATP-dependent transporters (Gatmaitan and Arias 1995; Borst and Elferink 2002). Among the most relevant transporters involved in bile formation are the bile salt export pump (Abcb11, also named Bsep), which transports mainly monoanionic bile salts, and the multidrug resistance-associated protein 2 (Abcc2, also named Mrp2), which transports a wide variety of anionic compounds including glutathione and glutathione conjugates (Gatmaitan and Arias 1995; Borst and Elferink 2002); these compounds contribute to the so-called bile salt-dependent fraction and salt-independent fraction of the bile flow, respectively (Esteller 2008).

Any alteration that affects the capacity of hepatocyte to produce bile leads to hepatocellular cholestasis. Estradiol-17 β -D-glucuronide (E17G) is among the compounds able to induce hepatocellular cholestasis. E17G is a D-ring endogenous metabolite of estradiol, and such compounds are increased during pregnancy (Adlercreutz et al. 1974), and may be a key factor in the pathogenesis of intrahepatic cholestasis (Vore et al. 1997) occurring in pregnant, susceptible women. E17G induces acute and reversible cholestasis in vivo, by impairing both fractions of bile flow (Crocenzi et al. 2003a). As a likely mechanism, E17G induces microtubule-independent endocytic internalization of both Abcb11 and Abcc2, and at the same time, inhibits microtubule-dependent dynamic reinsertion that occurs with canalicular transporters (Mottino et al. 2005).

Previous works demonstrated that E17G exerts its action through the activation of different signaling proteins that leads to transporter desinsertion (Abcb11, Abcc2) (Mottino et al. 2002, 2005; Crocenzi et al. 2003b). These signaling proteins are organized in several pathways. Up to now there are evidence that support that one of the pathways involves PKC, ER α , p38-MAPK, EGFR and Src, responsible for the initial endocytic internalization of canalicular transporters (Crocenzi et al. 2008; Boaglio et al. 2012; Barosso et al. 2012, 2015). On the other hand, E17G activates GPR30 that initiates two branches of signaling: in one branch, adenylyl cyclase/PKA start another pathway responsible for the initial endocytic internalization of transporters, in the other branch, phosphoinositide 3 kinase (PI3K)-Akt-MEK1/2-ERK1/2 participate in a pathway responsible for keeping transporters in a subapical space, restraining reinsertion (Boaglio et al. 2010, 2012; Zucchetti et al. 2014).

The insulin-like growth factor receptor-1 (IGF-1R) is a membrane-bound tyrosine kinase receptor that plays an important role in many biological processes. IGF-1 participates in estrogen-activated pathways. For example, sequential activation of IGF-1R and EGFR participates in estradiol stimulation of cell proliferation (Song et al. 2007) and additive or synergistic effects have been demonstrated with IGF-1R and ER α when both estradiol and IGF are administered simultaneously (Garcia-Segura et al. 2010).

Other signaling proteins that participate in E17G-induced cholestasis interact with IGF-1R. One example is PI3K (Miyata 2004). Diverse GPCRs plays a crucial role in the regulation of numerous physiological functions where IGF-1R is involved (Lappano et al. 2013), for example, the activation of ERK and Akt transduction pathways induced by IGF is regulated by GPCR kinases (Zheng et al. 2012). So far, IGF-1R can potentially interact with kinases and receptors activated by E17G (PI3K, GPR30, ER α , EGFR). In view of this, the aim of the present work is to evaluate if this receptor (IGF-1R) participates in E17G cholestasis and whether it is linked with pathways that involve GPR30 or ER α .

Materials

Cholyl-glycylamido-fluorescein (CGamF) was a generous gift from Prof. Alan Hofmann (University of California, San Diego). E17G, collagenase type A (from *Clostridium histolyticum*), 1-chloro-2,4-dinitrobenzene (CDNB), wortmannin (W), Leibovitz-15 (L-15) culture medium, G15, protease inhibitor cocktail, sodium taurocholate (TC), ICI182,780 (ICI), Alexa Fluor 568 phalloidin, 4,6-diamidino-2-phenylindole (DAPI) and 3- α -hydroxysteroid dehydrogenase were from Sigma Chemical Co. (St. Louis, MO). Tyrphostin AG1024 (TYR) was from Santa Cruz Biotechnologies (Dallas, TX). Dulbecco's modified Eagle medium (DMEM), Williams E medium, Hyperfilm ECL and Pierce ECL western blotting substrate were obtained from Thermo Fisher Scientific, Inc. (Waltham, MA). 5-chloromethylfluorescein diacetate (CMFDA) was obtained from Molecular Probes (Eugene, OR). Lipofectamine, TRIzol reagent, Superscript III Reverse Transcriptase, Platinum Taq DNA Polymerase, SYBR Green were from Life Technologies (Grand Island, NY). All the other reagents were of analytical grade.

Antibodies

Anti-Abcb11 antibody was from Kamiya Biomedical Co. (Seattle, WA, USA). Monoclonal antibody against human ABCC2 was from Alexis Biochemicals (San Diego, CA, USA). Phospho (Ser/Thr) Akt and total Akt were from Cell Signaling Technologies (Danvers, MA). Anti-phospho-insulin-like growth factor-1 receptor (pTyr1135/1136) and anti β -Actin antibody were from Sigma Chemical Co. Cy2-conjugated donkey anti-rabbit IgG and Cy2-conjugated goat anti-mouse IgG were from Jackson ImmunoResearch Laboratory (West Grove, PA, USA). Anti-Occludin antibody was from Zimed (Life Technologies, Grand Island, NY, USA).

Animals

Adult female Wistar rats weighing 250–300 g, bred in our animal house as described (Crocenzi et al. 2003b), were used in all studies under ketamine/xylazine anesthesia (100 mg/3 mg/kg of b.w., i.p). All animals received humane care according to the criteria outlined in the “Guide for the Care and Use of Laboratory Animals” Eighth Edition (National Academy of Sciences, 2011). Experimental procedures were carried out according to the local Guideline for the Use of Laboratory Animals (Faculty of Biochemical and Pharmaceutical Sciences, National University of Rosario, Argentina) established by the institutional Bioethical Committee for the Management of Laboratory Animals and the procedures were approved by the Faculty of Biochemical and Pharmaceutical Sciences of the National University of Rosario (Res 1074/2014 and 348/2016).

Isolation and culture of rat hepatocyte couplets (IRHC)

To obtain a preparation enriched in IRHC, livers were perfused according to the two-step collagenase perfusion procedure and were further enriched by centrifugal elutriation (Gautam et al. 1987; Wilton et al. 1991). The final preparation contained 70–80% of IRHC with viability > 95%, as assessed by the trypan blue exclusion test. After isolation, IRHCs were plated onto 24-well plastic plates at a density of 0.2×10^5 IRHC/mL in L-15 culture medium, and they were cultured for 5 h to allow the restoration of couplet polarity.

IRHC treatments

IRHCs were exposed to the vehicle (DMSO; control group) or E17G (25–400 μ M) for 20 min. This range of E17G concentrations is usually employed in rat-cell experiments (Boaglio et al. 2012; Barosso et al. 2012; Zucchetti et al. 2014). This concentration range was chosen taking into account the dose necessary to produce a decrease in bile flow. In an isolated perfused rat liver, the dose is 3 μ mol per liver, administered during a minute in a perfusing flow of 30 ml/min resulting in an approximate concentration of 100 μ M. Rat appears to be much more resistant to estrogen cholestasis than are humans (Vore 1987) and to get a reproducible effect on rat cells they have to be exposed to a concentration range probably higher than that found in serum or liver of women suffering from estrogen cholestasis.

To evaluate the role of IGF-1R in the effect of E17G, IRHCs were pre-incubated with the IGF-1R inhibitor TYR (100 nM) for 15 min, followed by the addition of E17G for another 20-min period. Then, to evaluate whether specific activation of IGF-1R was enough to reproduce E17G-induced cholestasis, cells were incubated only with the specific IGF-1R agonist, IGF-1 (0.1–20 nM), for 20 min. In

another set of experiments, IGF-1 (10 nM) was co-administered with EGFR agonist, EGF (10 nM), to try to reproduce E17G-induced alteration in transport activity.

To find out in which E17G-activated signaling pathway IGF-1R participates, studies of co-inhibition of ER α and IGF-1R were performed co-incubating ICI (1 μ M) together with TYR (100 nM) for 15 min before exposure to E17G (100 μ M) for another 20-min period. Similarly, studies of IGF-1R and PI3K co-inhibition were carried out by the co-incubation of IRHC with the PI3K inhibitor wortmannin (W, 100 nM) together with TYR (100 nM) for 15 min before exposure to E17G (100 μ M) for another 20-min period. To ascertain the role of microtubules in the protective effect of TYR, IRHCs were pretreated with the microtubule-disrupting agent colchicine (colch, 1 μ M) for 30 min and then exposed to E17G (100 μ M) for another 20-min period with or without a 15-min pretreatment with TYR.

To test whether IGF-1R activation follows that of PI3K or GPR30, cells was co-incubated with W (100 nM) or G15 (10 nM) together with IGF-1 (10 nM) for 15 min before exposure to E17G (100 μ M) for another 20 min. The experiment was repeated using insulin (10 nM or 1 μ M) instead of IGF-1 to test the specificity of the agonist in the process.

Assessment of Abcb11 and Abcc2 secretory function and localization in IRHC

For all studies, transport function of Abcc2 was evaluated by analyzing the canalicular vacuolar accumulation (cVA) of the fluorescent substrates glutathione methylfluorescein (GS-MF) (Roma et al. 2000). CMFDA is a lipophilic compound taken up by passive diffusion across the basolateral membrane and converted into glutathione methylfluorescein (GS-MF) by the sequential action of intracellular esterases and glutathione S-transferases. When necessary, transport function of Abcb11 was evaluated by analyzing the canalicular vacuolar accumulation (cVA) of the fluorescent substrates CGamF (Maglova et al. 1995; Wang et al. 2002). CGamF is a bile salt analog transported selectively by Abcb11 (Maglova et al. 1995).

For transport studies, cells were washed twice with L-15 and exposed to 0.3 μ M CGamF or 2.5 μ M CMFDA for 15 min. Finally, cells were washed twice with L-15, and canalicular transport activity for both substrates was assessed by fluorescence microscopy (Roma et al. 2000) under an inverted microscope (Zeiss Axiovert 25). Images were captured with a digital camera (Q-color5 Olympus America Inc., Center Valley, PA), and the cVA of the fluorescent substrates was determined as the percentage of IRHC in the images displaying visible green fluorescence in their canalicular vacuoles from a total analysis of at least 200 couplets per preparation.

To evaluate the intracellular distribution of Abcb11 and Abcc2, IRHCs were fixed and stained as previously reported (Barosso et al. 2012). E17G concentration used in these experiments (200 μ M) was higher than that employed in functional experiments to render transporter internalization more evident. The antibodies used were a polyclonal antibody against mouse Abcb11 (1:100) or a monoclonal antibody against human ABCC2 (1:100), followed by incubation with Cy2-conjugated donkey anti-IgG (1:200) or FITC-labeled goat anti-mouse IgG (1:200). To delimit the canaliculi, F-actin was stained with Alexa Fluor 568 phalloidin (1:100, 2 h). Cellular nuclei were stained by incubating during 10 min with 1.5 μ M DAPI. Cells were then mounted and examined with a Nikon C1 Plus confocal laser scanning microscope, attached to a Nikon TE-2000 inverted microscope.

Synthesis of siRNA

Four 21-nucleotide RNA duplexes (siRNA) targeting rat IGF-1R mRNA were designed using the WisiRNA selection program (Yuan et al. 2004) taking into account that the selected siRNAs do not target insulin receptor that share homology with IGF-1R. The control siRNA (scrambled) was designed by scrambling the nucleotides of one of these specific targets. The siRNAs were synthesized using the Ambion's Silencer™ siRNA Kit. siRNA1, siRNA2, siRNA3 and siRNA4 targeting rat IGF-1R nucleotides are: 2930-2951 (5'AAGAGGAATAACAGCAGATTG3'), 4613-4634 (5'AAATTGACTTAATGGCTGCC3'), 636-657 (5'AAC AATGAGTACAACCTACCGC3') 1505-1526 (5'AACCTG TGAAAGTGATGTTCT3').

IGF-1R knock-down in sandwich-cultured rat hepatocytes

Hepatocytes were isolated from female Wistar rats as was described previously (Garcia et al. 2001), seeded (9.5×10^5 cells/well) onto six-well plates covered with gelled collagen (800 μ L of rat tail collagen type I mixed with 100 μ L of 0.1 M NaOH and 100 μ L of 10 \times DMEM) and incubated for 2 h at 37 °C in Williams E medium with FBS 5% containing antibiotics (gentamicin, streptomycin, penicillin and amphotericin D), dexamethasone 0.8 mg/L, and insulin 4 mg/L. Afterwards, the medium was replaced and cells were incubated for 24 h before transfection.

We optimized transfection of primary hepatocytes by adding 5 μ L of lipofectamine with 70 nM of siRNA per well, followed by a 6-h incubation at 37 °C. After transfection, hepatocytes were washed and overlaid with gelled collagen for 1 h at 37 °C to obtain a collagen sandwich configuration (Barosso et al. 2012). After 48 h of culture in sandwich configuration, total RNA was isolated using Trizol reagent

and IGF-1R mRNA levels were determined. cDNA was synthesized from 1 μ g of total RNA with the Superscript III Reverse Transcriptase using random hexamers according to manufacturer's instructions. Real-time PCR reactions were carried out on a MX3000P system (Agilent Technologies, Santa Clara, CA, USA) with Platinum Taq DNA Polymerase. The amount of template was quantified with SYBR Green. Primers were used at a final concentration of 1 μ M. Primer sequences were: IGF-1R (1073, F) 5'ATTCTGTGACGTCTGCCAG3' and IGF-1R (1214, R) 5'TTCACGTAGCCAGTCACCAC3'. The thermal protocol was 95 °C for 10 min followed by 40 cycles of 95 °C for 15 s, 59 °C for 30 s and 72 °C for 30 s. Relative levels of IGF-1R normalized to GAPDH mRNA were calculated based on the $2^{-\Delta C_t}$ method (Pfaffl et al. 2002; Zucchetti et al. 2014). Specificity of each reaction was verified with a dissociation curve between 55 and 95 °C with continuous fluorescence measure. siRNA2 produced a significant decrease in IGF-1R mRNA level. Hence, siRNA2 was chosen in the studies of IGF-1R knock-down, (see Fig. 4).

Assessment of Abcc2 and Abcb11 localization and secretory function in hepatocytes cultured in collagen sandwich

To evaluate the intracellular distribution of Abcc2 and Abcb11, SCRH were treated with E17G (200 μ M, 20 min) or vehicle (DMSO, control) and then fixed with 4% paraformaldehyde in PBS for 30 min, blocked and permeabilized with 3% BSA and 0.5% Triton X-100 for 30 min. After that, cells followed the same procedure indicate for IHRC for the incubation with primary and secondary antibodies. At least three areas of confluent cells from each culture dish were randomly examined by confocal microscopy.

Assessment of Abcc2 secretory function in hepatocytes cultured in collagen sandwich

The functional status of Abcc2 was evaluated by determination of the pseudocanalicular accumulation of GS-MF, as previously described (Miszczuk et al. 2015). In brief, CMFDA was added to the medium and time-lapse imaging was done every minute during 8 min with a fluorescence microscope. Between 70 and 100 pseudocanaliculi were selected in each image, and the average of time fluorescence of GS-MF was measured. The slope of the line was estimated as a measure of initial transport rate (ITR).

Isolation and culture of rat hepatocytes

Isolated hepatocytes were obtained by collagenase perfusion, and cultured in 3-cm Petri dishes at a density of 2×10^6

cells/mL (Garcia et al. 2001). After a 24-h culture period, cells were subjected to treatments.

Immunoblot analysis of IGF-1R phosphorylation

The activation of IGF-1R was confirmed evaluating the phosphorylation in the Tyr-1135-36 amino acid (Kato et al. 1994) via western blotting in hepatocyte primary cultures. Cells were exposed to DMSO (control) or E17G (100 μ M) for 15 min, in the presence or absence of G15 (10 nM) for experiment activation sequence. Then, cells were lysed and western blot was performed (Barosso et al. 2015). Membranes were first exposed overnight to anti (p-Tyr-1135-36) IGF-1R antibody (1:1000) and revealed, then stripped and re-probed with an anti-actin antibody (1:1000). pIGF-1R and actin bands were quantified by densitometry with ImageJ 1.48.

Immunoblot analysis of Akt phosphorylation

The activation of PI3K was confirmed by evaluating the phosphorylation status of Akt, a final PI3K effector, via western blotting.

Cells were exposed to DMSO (control) or E17G (100 μ M) for 15 min, in the presence or absence of TYR. Then, cells were lysed and western blot was performed (Barosso et al. 2015). Membranes were first exposed overnight with an anti (p-Ser-473) Akt antibody (1:2000). The membranes were then stripped and re-probed with an anti-total Akt antibody (1:1000). p-Akt and total Akt bands were quantified by densitometry with ImageJ 1.48.

Isolated perfused rat liver (IPRL)

In anesthetized female rats, the bile duct was cannulated with PE-10 tubing (Intramedic, BD, Franklin Lakes, NJ, USA). Livers were perfused in situ via the portal vein in a non-recirculating single-pass design with Krebs–Ringer bicarbonate at 37 °C, equilibrated with 5% CO₂/95% O₂, at a constant flow rate of 30 mL/min. Taurocholate (2.5 μ mol/L) and 1-chloro-2,4-dinitrobenzene (CDNB, 0.5 μ mol/L) were added to the perfusion medium for bile salt and DNP-glutathione secretion studies. After a 20-min equilibration period, the inhibitor TYR (100 nM final concentration) or its solvent (DMSO, 370 μ L/L) was added to the reservoir. Fifteen minutes later, a 5-min basal bile sample was collected, followed by administration of E17G (3 μ mol/liver, intraportal single injection over a 1-min period) or its solvent (DMSO/10% BSA in saline), and bile was collected at 5-min intervals for an additional 40-min period. Experiments were considered valid only if initial bile flow (after equilibration) was greater than 30 μ L/min/kg. Viability of the liver was monitored via lactate dehydrogenase activity in the perfusate outflow; experiments exhibiting activities

over 20 U/L were considered invalid. Transport activities of Abcc2 and Abcb11 were evaluated by measuring biliary DNP-glutathione and taurocholate excretion, respectively. DNP-glutathione content was assessed in all samples by high-performance liquid chromatography, as described previously (Mottino et al. 2001), using authentic standards. Total bile salt concentration was assessed using the 3 α -hydroxysteroid dehydrogenase procedure (Barosso et al. 2012; Zucchetti et al. 2014) and the result was assumed as TC concentration.

For canalicular transporter localization studies, in a new set of experiments, a liver lobe was excised 40 min after the addition of E17G, frozen immediately in isopentane pre-cooled in liquid nitrogen, and stored at – 70 °C for further immunofluorescence and confocal microscopy analysis. Liver sections were obtained with a Zeiss Microm HM500 microtome cryostat, air-dried, and fixed with 3% paraformaldehyde in phosphate-buffered saline for co-localization studies. After fixation, liver slices were incubated overnight with the specific antibodies to Abcb11, Abcc2, and occludin, and this was followed by 1 h of incubation with the appropriate cyanine 2-conjugated or cyanine 3-conjugated donkey anti-IgG. Occludin staining was carried out to demarcate the limits of the canaliculi (Misra et al. 2003; Donner et al. 2007). All images were taken with a Nikon C1 Plus confocal laser scanning microscope. To ensure comparable staining and image capture performance for the different groups belonging to the same experimental protocol, liver slices were on the same day, mounted on the same glass slide, and subjected to the staining procedure and confocal microscopy analysis simultaneously. Image analyses of the degree of Abcb11 and Abcc2 endocytic internalization were performed on confocal images with ImageJ 1.48 (National Institutes of Health), as described elsewhere (Barosso et al. 2012; Zucchetti et al. 2013).

Statistical analysis

Results are expressed as mean \pm standard error of the media (SEM). One-way ANOVA, followed by Newman–Keuls' test, was used for multiple comparisons. The four-parameter dose–response curves were compared using GraphPad Prism software (GraphPad Software Inc., La Jolla, CA, USA). Values of $p < 0.05$ were considered to be statistically significant.

Results

IGF-1R participates in E17G-induced impairment of canalicular secretory function

To characterize the role of IGF-1R, we carried out concentration–response studies in which the concentration of

E17G was modified in the presence of a fixed concentration of the inhibitor TYR (100 nM) (Fig. 1). Curves were adjusted assuming that the parameter minimal effect (bottom) was equal to 100% (similar to control) and that the Hill slope coefficient was 1. TYR significantly prevented E17G-induced decreases in cVA of GS-MF (Fig. 1a) and CGamF (Fig. 1b) since there was a shift of the curve to the right. IC₅₀ of GS-MF and CGamF accumulation induced by E17G (114 ± 10 and 107 ± 8 μ M, respectively, $n = 3$) were significantly increased in the presence of TYR by 296 and 178%, (E17G+TYR, IC₅₀: 338 ± 58 μ M, E17G+TYR 191 ± 14 μ M, $p < 0.05$, $n = 3$).

Additionally, experiments with the specific IGF-1R agonist, IGF-1 (0.1–20 nM), show that this treatment did not modify cVA of GS-MF, as compared to the control, thus

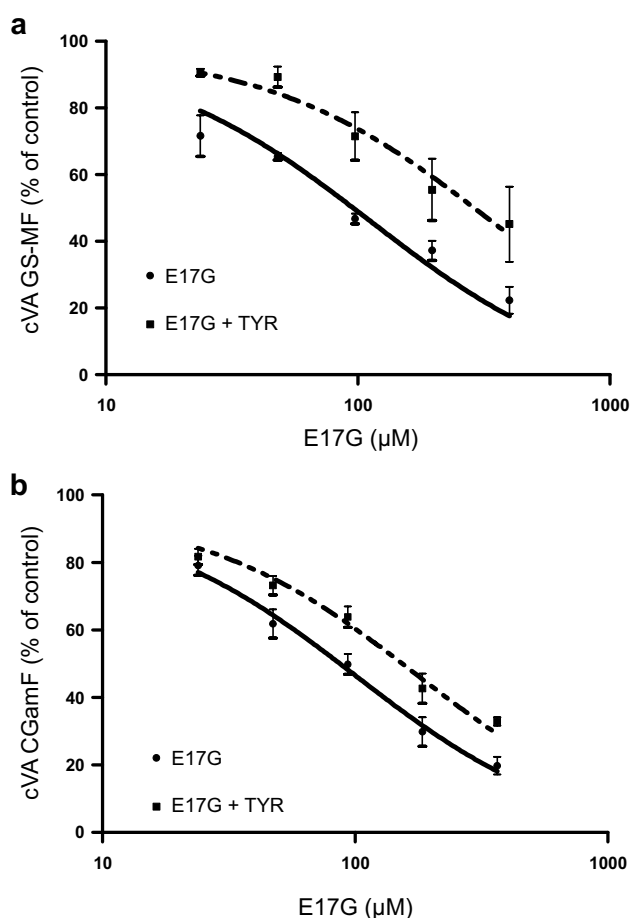


Fig. 1 Prevention by tyrphostin AG1024 (TYR) of estradiol 17 β -D-glucuronide (E17G)-induced impairment of canalicular vacuolar accumulation (cVA) of GS-MF (a) and CGamF (b). IRHCs were pre-incubated with TYR (100 nM) for 15 min, and then exposed to E17G (25–400 μ M) for an additional 20-min period. cVAs of CGamF and GS-MF were calculated as the percentage of couplets displaying visible fluorescence in their canalicular vacuoles from a total of at least 200 couplets per preparation, referred to control cVA values. Data are expressed as mean \pm SEM ($n = 3$)

indicating that the activation of IGF-1R is necessary but not sufficient to impair canalicular secretory function of Abcc2 (see Additional Fig. 1a).

TYR prevented E17G-induced internalization of canalicular transporters Abcb11 and Abcc2

Internalization of Abcc2 and Abcb11 was analyzed in immunostained IHRC with a confocal laser scanning microscope. Confocal images in Fig. 2 show that E17G produces a redistribution of Abcc2 (Fig. 2a) and Abcb11 (Fig. 2b) from the canalicular membrane into intracellular vesicles (arrows). The pretreatment of IRHCs with TYR markedly prevented this delocalization. Neither E17G nor Tyr treatment modified actin distribution.

Knock-down of IGF-1R prevents both, the impairment of Abcc2 transport activity and the endocytic internalization of transporters induced by E17G

To confirm the participation of IGF-1R in E17G-induced cholestasis alteration, we evaluated Abcc2 transport function and the localization status of Abcc2 and Abcb11 in SCRH transfected with siRNA targeting rat IGF-1R mRNA. Four different siRNAs were tested; among them, siRNA2 produced a significant decrease in IGF-1R mRNA level (see Fig. 3a) and it was chosen to study Abcc2 function in SCRH.

Figure 3b shows that IGF-1R knock-down prevented the functional alteration induced by E17G measured by initial transport rate (ITR) of GS-MF. The same figure (panel c) presents representative confocal images that show that E17G-induced internalization of Abcc2 (arrows) was prevented by IGF-1R knock-down, giving additional support to a role of IGF-1R in E17G-induced actions. Cells treated with scrambled siRNA showed the same delocalization pattern of Abcc2 as E17G. The same phenomenon was observed for the immunofluorescence images of the transporter Abcb11 (Fig. 3d).

IGF-1R does act complementarily with ER α but not with PI3K, in the E17G-induced canalicular secretory failure

The preventive effects of ICI (1 μ M) and TYR (100 nM) on the decrease in cVA of GS-MF (Fig. 4a) and CGamF (Fig. 4b) induced by E17G were lesser in magnitude than the effect produced together. On the other hand, the preventive effects of TYR (100 nM), W (100 nM) and both simultaneously produced similar protection on the decrease in cVA of GS-MF (Fig. 5a) and CGamF (Fig. 5b) and in the case of GS-MF this effect was reversed in the presence of Colch (Fig. 5c). This suggests that IGF-1R acts in the same pathway of PI3K: their conjoint

Fig. 2 Insulin-like growth factor receptor-I inhibitor tyrphostin AG1024 (TYR) prevented estradiol 17 β -D-glucuronide (E17G)-induced endocytic internalization of Abcc2 and Abcb11 in IRHC. **a** Representative confocal images depicting cellular distribution of the canalicular Abcc2 under the different treatments. Note that under control or TYR conditions transporter-associated fluorescence is mainly localized at the canalicular membrane. E17G (200 μ M) induced a clear internalization of transporter-containing vesicles beyond the limits of the canaliculus (arrows), phenomenon significantly prevented by pretreatment with TYR (100 nM, 15 min). The same phenomenon was observed for the immunofluorescence images of the transporter Abcb11 (**b**). The densitometric analysis of the modification of the distribution of Abcc2 and Abcb11 by the different treatments is presented as additional Fig. 2

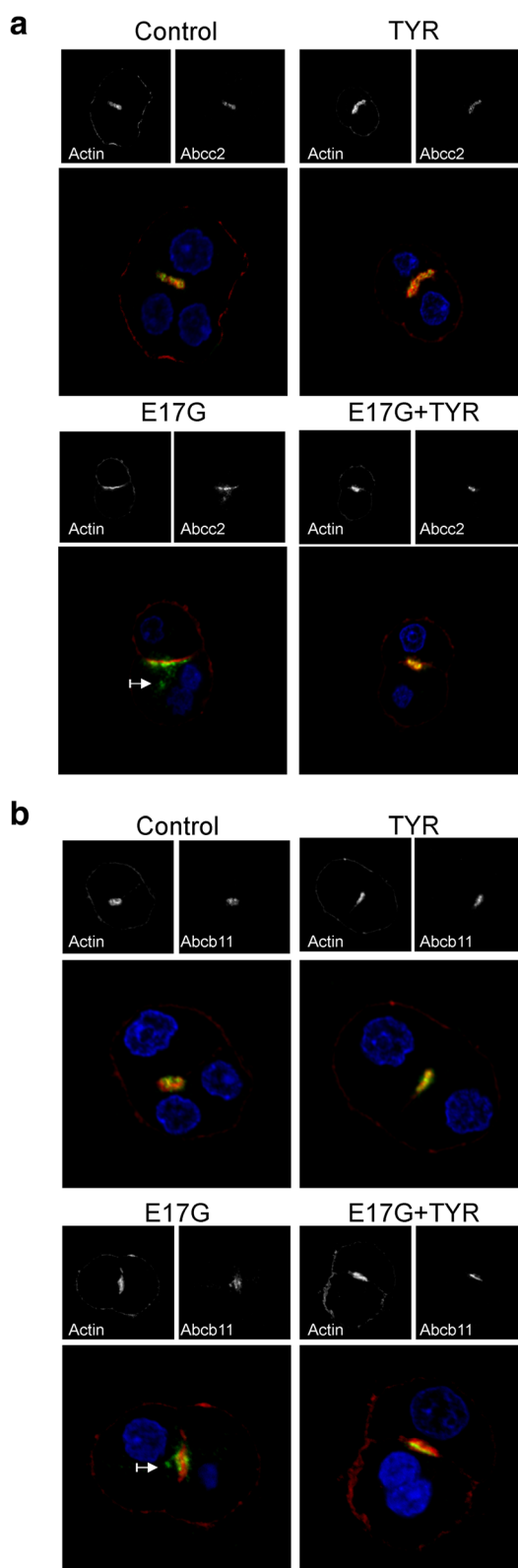
inhibition did not sum protection and both protective effects depend on the polymerization of microtubules. It is worth noting that the concentration of the inhibitors employed produced the maximal protective effects allowing us to speculate about summing protective effects.

IGF-1R activation is downstream of GPR30 and upstream of that of PI3K-Akt

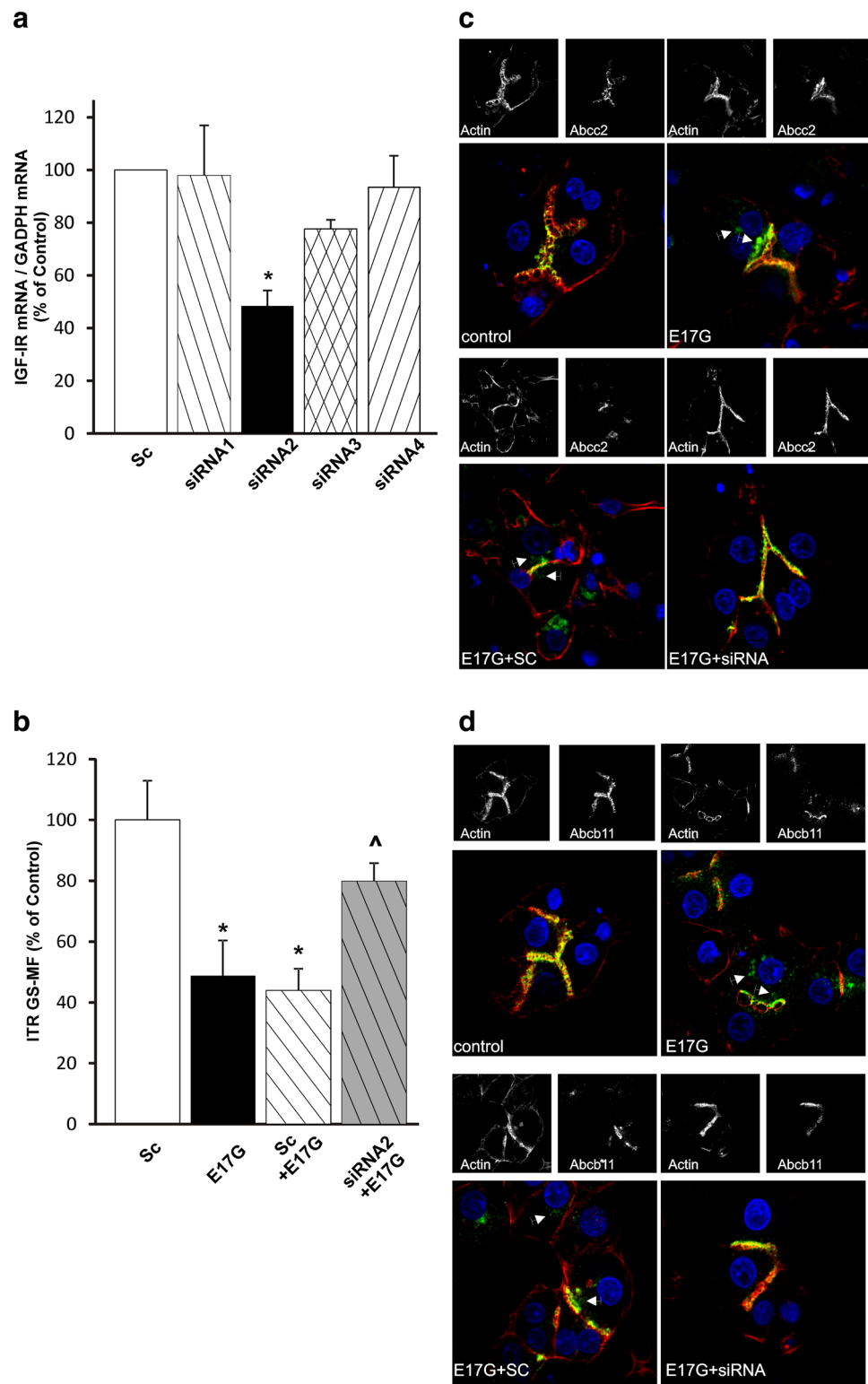
To evaluate the order in the sequential activation of IGF-1R, GPR30 and PI3K/Akt, two different experiments were performed (Fig. 6). First, western blots of p-IGF-1R (Tyr-1135-36), an indicator of IGF-1R activation, showed the increased amount of p-IGF-1R (Fig. 6a) by E17G. Figure 6a shows that this increase reached a peak at 15 min and it was decreased in the presence of G15, indicating that IGF-1R activation follows that of GPR30. Second (Fig. 6b), pretreatment with TYR prevented the phosphorylation of Akt (p-Ser-473, an estimate of the activation of PI3K), induced by E17G indicating that the activation of IGF-1R precedes PI3K/Akt activation.

IGF-1 decreases the protection produced by G15 but not that produced by wortmannin in the E17G-induced canalicular secretory failure

To confirm the temporal activation of IGF-1R, GPR30 and PI3K, we employed a different approach using the specific ligand IGF-1. If IGF-1R activation follows the activation of another protein, when this other protein is inhibited, IGF-1 would restore the action of E17G, whereas if the activation of the other protein follows that of IGF-1R, IGF-1 would not restore the action of E17G when the other protein is inhibited. G15 prevented the decrease in cVA of GS-MF induced by E17G and this prevention was partially abolished by IGF-1 (Fig. 7b), whereas IGF-1 did not affect the protection of W in the E17G-induced canalicular secretory failure (Fig. 7a), indicating that IGF-1R activation occurs after that GPR30 and before that PI3K activation. Figure 8b confirms that the “restorative” effect is specific of IGF-1;



insulin, which has some overlapping effects with IGF-1, did not affect G15 prevention of the decrease in cVA of GS-MF induced by E17G.



Subsequently, IGF-1R is proposed to be in a pathway downstream of GPR30, and EGFR is in another pathway, downstream of ER α ; we tested the conjoint action of IGF-1 and the EGFR agonist, EGF. The simultaneous action of both agonists did not induce a canalicular

secretory failure, indicating that activation of both pathways is not sufficient to produce cholestatic effects (Additional Fig. 1b).

Fig. 3 Insulin-like growth factor receptor-I (IGF-1R) knock-down in sandwich-cultured rat hepatocytes. **a** Graphic depicts the relative levels of IGF-1R mRNA normalized to GAPDH mRNA based on the $2^{-\Delta\Delta Ct}$ method. siRNA1, siRNA2, siRNA3 and siRNA4 targeting rat IGF-1R nucleotides are 2930-2951 (5' AAGAGGAATAACAGCAGATTG3'), 4613-4634 (5' AAATTGACTTAATGGCTGCC3'), 636-657 (5' AACAAATGAGTACAACACTACCGC 3') and 1505-1526 (5' AACCTGTGAAAGTGATGTTCT 3'). The siRNA2 produced a significant decrease in IGF-1R mRNA level. Results are referred as percentage of scrambled (Sc) and expressed as mean \pm SEM ($n = 3$). *Significantly different from control. **b** SCRHs were transfected with specific siRNA or scrambled for 48 h and then exposed to E17G (200 μ M) for 30 min. The slope of the curve obtained by plotting the average GS-MF-associated fluorescence of 70–100 pseudocanaliculi versus time was used to estimate the ITR of Abcc2. Data are expressed as mean \pm SEM ($n = 3$), *significantly different from scrambled, ^significantly different from scrambled and E17G, ($p < 0.05$, $n = 3$). **c, d** Representative confocal images showing cellular distribution of Abcc2 (**c**) (green) and Abcb11 (**d**) (green) in SCRH under different treatments. Actin network (red) and nuclei (blue) are also shown. Under control conditions, Abcc2 and Abcb11 associated fluorescence is mainly localized at the canalicular membrane in the area delimited by the pericanalicular actin network. E17G induced a clear internalization of transporter-containing vesicles beyond the limits of the pericanalicular actin (indicated by arrowheads). In cells treated with siRNA2 this phenomenon was significantly prevented. Scrambled-transfected cells also showed a pattern of Abcc2 and Abcb11 delocalization after E17G treatment. None of the treatments affected the normal distribution of actin, which showed a predominant pericanalicular distribution (color figure online)

IGF-1R is involved in the decay of bile secretory function induced by E17G in the IPRM model

The IPRM model allows us to study the dynamic follow-up of changes in the function of biliary secretion produced by the administration of E17G. The endocytosis of the transporters that causes the acute reduction of biliary flow and the subsequent recovery due to reinsertion of these transporters occur differentially over time.

E17G bolus administration decreased biliary flow to a minimum of approximately 40% in 10 min, and biliary flow did not recover throughout the perfusion period (Fig. 8a). This was accompanied by a decrease in biliary excretion of the substrates Abcc2 and Abcb11, DNP-glutathione (minimum 15%, Fig. 8b) and taurocholate (minimum 35%, Fig. 8c), respectively. TYR (100 nM) had no effect on this initial drop, whereas TYR accelerated the recovery of biliary flow at 15 min after the administration of E17G. On the other hand, biliary excretion of DNP-G and taurocholate improved 25 min after administration of E17G where DNP-G excretion reached a minimum of 60% and taurocholate reached a minimum of 80%.

Figure 9 shows that in control livers, the fluorescence associated with the transporter was limited to the canalicular space; the same phenomenon was observed in TYR-treated rat livers. In E17G-treated livers, relocalization of intracellular fluorescence associated with both carriers from the

canalicular space to the pericanalicular area was apparent, as indicated by the decrease in the fluorescence intensity in the canalicular area together with the increased fluorescence at a greater distance from the canalculus; this indicates endocytic internalization of the carriers whereas TYR extensively prevented the internalization of Abcc2 and Abcb11 (densitometric analysis of immunofluorescence images is presented in Additional Fig. 3). This supports our contention that IGF-1R contributes to E17G-induced cholestasis by retargeting of the endocytosed transporters.

Discussion

This work describes how IGF-1R, a receptor mainly involved in glucose and lipid metabolism, is involved in estradiol-17 β -D-glucuronide (E17G)-induced endocytic internalization of Abcb11 and Abcc2, and how IGF-1R interacts with other proteins, providing further insights into the intracellular signaling pathways involved in E17G-induced cholestasis.

The IGF-1R consists of a 400 kDa $\alpha_2\beta_2$ heterotetramer complex with two extracellular α subunits containing ligand binding sites. Each α -subunit of IGF-1R can be coupled to one of two membrane spanning subunits containing domains with intrinsic tyrosine kinase activity (Troncoso et al. 2014). IGF-1, ligand of IGF-1R, is an anabolic insulin-like growth hormone with an essential role in cell proliferation, growth and metabolism, and it is associated with the prevalence of pathologies such as obesity and aging (Franco et al. 2006; Troncoso et al. 2014). The binding of IGF-1 to the receptor results in the autophosphorylation of specific cytosolic tyrosine residues within the IGF-1R receptor, increasing the activation of its intrinsic tyrosine kinase activity and leading to the phosphorylation of intracellular substrates. The phosphorylation of IGF-1R triggers the activation of a variety of signaling proteins including, PI3K (Suleiman et al. 2007) and the heterotrimeric G protein, G_{i2} , which is coupled to activation of the Erk1/2 pathway (Kuemmerle and Murthy 2001).

Our group has shown that GPR30, a GPCR, and ER α accounts in part for the acute cholestasis caused by E17G (Barosso et al. 2012; Zucchetti et al. 2014), event that correlates well with the ability of the estrogen to induce endocytic internalization of the canalicular transporters such as Abcc2 and Abcb11 (Mottino et al. 2003, 2005). The actions of GPR30 and ER α in E17G-induced cholestasis constitute different independent pathways. Our group also described the activation of PI3K in the GPR30 pathway and the activation of cPKC in the ER pathway (Boaglio et al. 2010; Barosso et al. 2012; Zucchetti et al. 2014). Recently, our group has demonstrated that EGFR participates downstream of ER α and upstream of Src family protein kinases (Barosso et al. 2015).

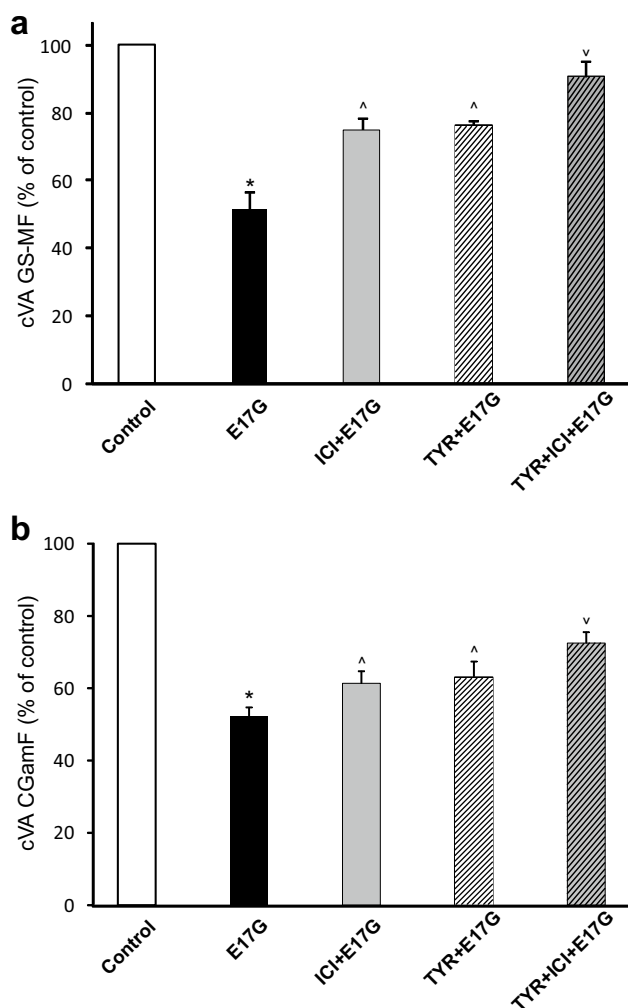


Fig. 4 Effect of co-incubation with tyrphostin AG1024 (TYR) and estrogen receptor α (ER α) inhibitor (ICI) on estradiol 17 β -D-glucuronide (E17G)-induced impairment of canaliculular vacuolar accumulation (cVA) of GS-MF and CGamF. IRHCs were incubated with ICI (ER α inhibitor, 1 μ M) and TYR (100 nM), either alone or together, for 15 min. Then, IRHCs were exposed to E17G (100 μ M) for an additional 20-min period. Finally, cVAs of GS-MF (a) or CGamF (b) were calculated as the percentage of couplets displaying visible fluorescence in their canaliculular vacuoles from a total of at least 200 couplets per preparation, referred to control cVA values. Data are expressed as mean \pm SEM ($n = 3$). *Significantly different from control ($p < 0.05$). ^Significantly different from E17G and control ($p < 0.05$). ^vSignificantly different from E17G, TYR + E17G and ICI+E17G ($p < 0.05$)

The role of IGF-1R in E17G-induced cholestasis was evaluated in vitro and in IPRL using different approaches to evaluate transport function, transporter localization and protein activations. The participation of IGF-1R was evaluated using the inhibitor TYR and specific siRNA to knock-down the receptor. Concentration–response experiments showed that TYR displaced the E17G concentration–response curve of cVA of Abcc2 substrate and Abcb11 substrate to the right,

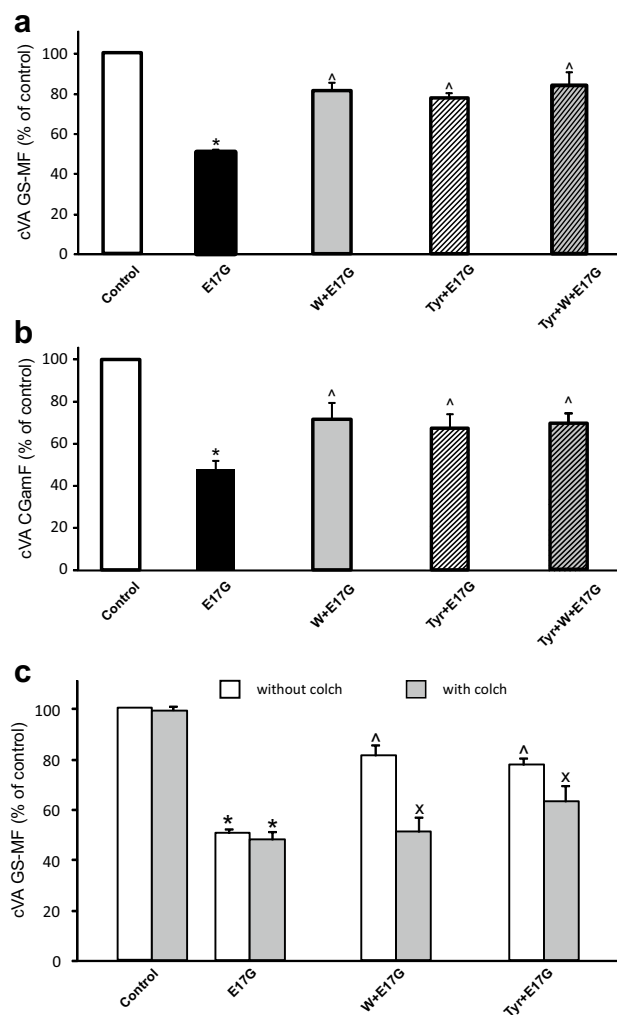


Fig. 5 Effect of co-incubation with tyrphostin AG1024 (TYR) and PI3K inhibitor (W) on estradiol 17 β -D-glucuronide (E17G)-induced impairment of canaliculular vacuolar accumulation (cVA) of GS-MF and CGamF. a, b IRHCs were incubated with wortmannin (W, PI3K inhibitor, 100 nM) and TYR (100 nM), either alone or together, for 15 min. Then, IRHCs were exposed to E17G (100 μ M) for an additional 20-min period, finally cVAs GS-MF (a) or CGamF (b) were calculated as the percentage of couplets displaying visible fluorescence in their canaliculular vacuoles from a total of at least 200 couplets per preparation, referred to control cVA values. c IRHCs were incubated with W and TYR with or without Colchicine (Colch, 1 μ M). Then, IRHCs were exposed to E17G (100 μ M) for an additional 20-min period, finally cVAs GS-MF was calculated as the percentage of couplets displaying visible fluorescence in their canaliculular vacuoles from a total of at least 200 couplets per preparation, referred to control cVA values. Data are expressed as mean \pm SEM ($n = 3$). *Significantly different from control ($p < 0.05$). ^Significantly different from E17G and control ($p < 0.05$). ^xSignificantly different from “without colch” ($p < 0.05$)

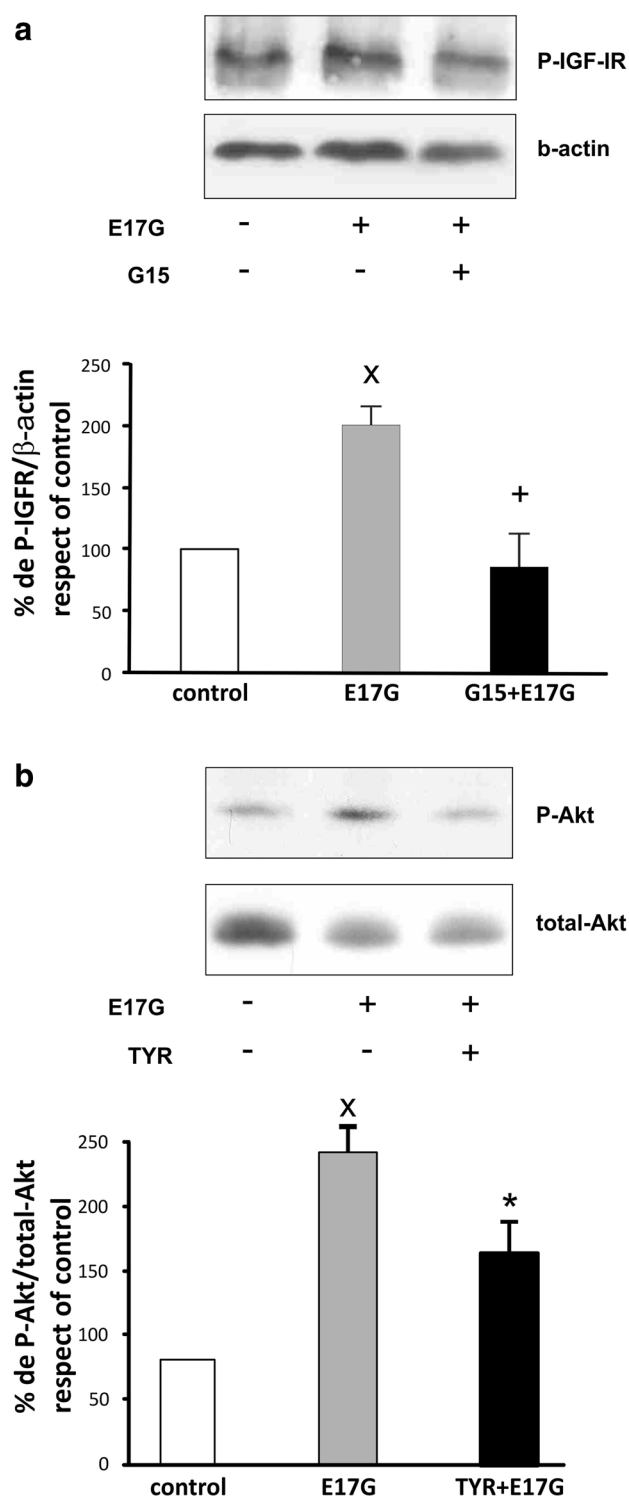
indicating a partial protective effect of these compounds on the cholestasis induced by E17G. Protection was confirmed with knock-down experiments in SCRHCs where cells transfected with siRNA for IGF-1R presented a significantly

Fig. 6 Activation IGF-1R and PI3K/Akt in the presence of the corresponding cross inhibitors. **a** Effect of G15 (GPR30 inhibitor) on the specific IGF-1R activation by E17G in primary cultured hepatocytes. Primary cultured hepatocytes were treated with G15 (10 nM) for 15 min, then exposed to E17G (100 μ M) for 15 min, and finally IGF-1R activity was determined by immunoblots using antibodies against phosphorylated IGF-1R (p-IGF-1R, Tyr-1135-36) and β -actin. The ratio of each p-IGF-1R/ β -actin band density was compared to control bands ratio (100%). **b** Effect of TYR on PI3K/Akt activation by E17G. Isolated rat hepatocytes were incubated with TYR (100 nM) for 15 min and the exposed to E17G (100 μ M) for another 15 min period. PI3K/Akt activity was determined by immunoblots using antibodies against phosphorylated Akt (p-Akt, Ser473) and total Akt. The ratio of each p-Akt/total Akt band density was compared to control bands ratio (100%). Data are expressed as mean \pm SEM ($n = 3$). [‡]Significantly different from control ($p < 0.05$). *Significantly different from E17G and E17G ($p < 0.05$). [†]Significantly different from E17G ($p < 0.05$)

lower decrease in the initial transport rate of GS-MF after being treated with E17G. Western blot studies demonstrate that E17G treatment increase IGF-1R phosphorylation in Tyr-1135-36, placing the receptor in a pathway activated by the estrogen. Confocal images indicated that IGF-1R participates also in the delocalization of Abcc2 and Abcb11; both the inhibitor and the knock-down of the receptor prevented internalization of the transporters, as seen in the images and quantified by densitometric analysis (Additional Fig. 2).

The role of IGF-1R in the effects of E17G on transport activity and transport delocalization was not only demonstrated in vitro but also in a more complex physiological model such as IPR in which the phenomena of canalicular transporters internalization and retrieval can be differentiated. TYR did not prevent the initial effect of E17G on bile flow and on the excretion of TC (Abcb11 substrate) and DNP-G (Abcc2 substrate), but conversely, TYR improved the recovery of these parameters, indicating that the pathway in which the IGF-1R participates affects the spontaneous reinsertion of canalicular transporters.

There are evidence that support that E17G activates three pathways; one that involves ER α , PKC, p38-MAPK, EGFR and Src is responsible for the initial endocytic internalization of canalicular transporters (Crocenzi et al. 2008; Boaglio et al. 2012; Barosso et al. 2012, 2015), the other two pathways initiate in GPR30, one involves AC, PKA and is also responsible for endocytic internalization of canalicular transporters (Zucchetti et al. 2014) and the other involves PI3K-Akt, MEK/ERK which is responsible for keeping transporters in a subapical space, restraining reinsertion (Boaglio et al. 2010; Zucchetti et al. 2014). Once established the participation of IGF-1R in E17G induced cholestasis, our aim was to locate IGF-1R in one of the pathways activated by E17G and to propose a sequence of activation with the other proteins in the pathway. IGF-1R and ER α co-inhibition produced an additive preventive effect, suggesting that they belong to different pathways, whereas IGF-1R and PI3K



co-inhibition was not additive, suggesting that they share a common pathway. Colchicine abolished the protection produced by TYR similarly to what was previously observed with wortmannin (inhibitor of PI3K) (Boaglio et al. 2010). On the other hand, through the combination of the inhibition of one protein and the measurement of the other protein

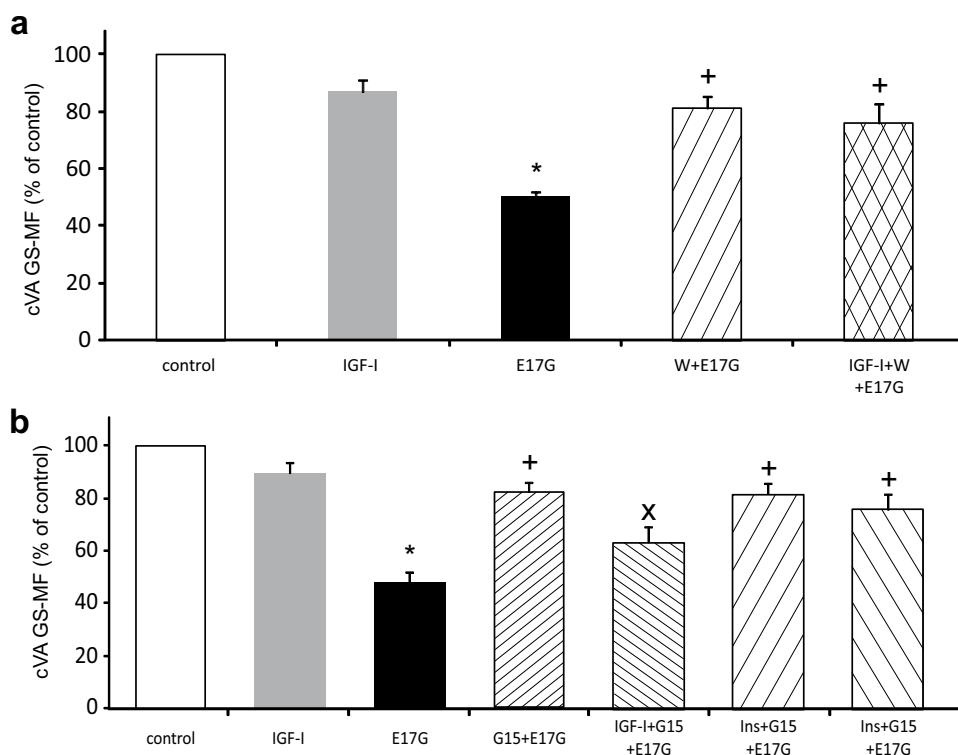


Fig. 7 Experiments to elucidate the possible sequence by which IGF-1R participates in E17G-induced canalicular secretory failure. **a** IRHCs were pretreated with wortmannin (W, 100 nM) and IGF-1 (10 nM) for 15 min and followed by treatment with E17G (100 μ M) for 20 min. Finally, IRHCs were exposed to CMFDA (2.5 μ M) for 15 min, and cVA of GS-MF was calculated as the percentage of couplets displaying visible fluorescence in their canalicular vacuoles from a total of at least 200 couplets per preparation, referred to as control cVA values. *Significantly different from control ($p < 0.05$); +significantly different from E17G and control ($p < 0.05$); Xsignificantly different from E17G and control ($p < 0.05$). Data are expressed as mean \pm standard error of the mean (SEM; $n = 3$). **b**

IRHCs were pretreated with G15 (10 nM), IGF-1 (10 nM) or insulin (10 nM, 1 μ M) for 15 min and followed by treatment with E17G (100 μ M) for 20 min. Finally, IRHCs were exposed to CMFDA (2.5 μ M) for 15 min, and cVA of these fluorescent substrates was calculated as the percentage of couplets displaying visible fluorescence in their canalicular vacuoles from a total of at least 200 couplets per preparation, referred to as control cVA values. *Significantly different from control ($p < 0.05$); +significantly different from E17G and control ($p < 0.05$); Xsignificantly different from G15+E17G ($p < 0.05$). Data are expressed as mean \pm standard error of the mean (SEM; $n = 3$)

activation by western blot, experiments demonstrated that IGF-1R activation occurs after that of GPR30 and preceded that of PI3K. Confirming this sequence, the activation of IGF-1R with IGF-1 reversed the prevention observed in cells treated with E17G when GPR30 was inhibited with G15. Results of IPRL are consistent with the placement of IGF-1R in the same pathway of PI3K since the pattern of lack of action of the inhibitor (TYR) in the initial phase of E17G action and the accelerated recovery after reaching the nadir of bile flow and substrate excretion are similar to those obtained with inhibitors of PI3K (Boaglio et al. 2010) and ERK (Boaglio et al. 2012).

Since IGF-1R can be activated by its agonist IGF, we tested whether IGF-1R activation alone could affect canalicular transport activity. IGF per se could not alter GS-MF transport, neither the combination of IGF with EGF, an EGFR specific agonist, which together activate two of the three pathways branches described so far. Previously, we

demonstrated that the simultaneous activation of GPR30 by G1 and EGFR by EGF provoke a significant decrease in Abcc2 transport activity (Barosso et al. 2015). The difference between both experiments is that G1+EGF activate the three pathway branches that are activated by E17G instead of the two activated by IGF+EGF (see Fig. 10 were the pathways activated by E17G are depicted). This is in line with the hypothesis that the activation of the three pathways by E17G is necessary to fulfill a significant delocalization of canalicular transporters.

The mechanism by which GPR30 activates IGF-1R in the presence of E17G results elusive because of our poor knowledge on the molecular mechanisms that trigger this process, but several reports in other cell models provide some hints in that metalloproteinases (Song et al. 2007) could participate releasing IGF from an extracellular source.

Garcia-Regalado et al. proposed a model of activation of PI3K by G protein couple receptors in which it would

Fig. 8 Tyrphostin AG1024 (TYR) protects against estradiol-17 β -D-glucuronide (E17G)-induced impairment of bile flow and biliary secretion of dinitrophenyl-glutathione and taurocholate in the perfused rat liver. Temporal changes in bile flow (a) and in the biliary excretion rate of both total dinitrophenyl-glutathione (DNP-G, b) and taurocholate (c) throughout the perfusion period. IPRs were treated with a bolus of E17G (3 μ mol/liver) or with the E17G vehicle DMSO/BSA 10% in saline (control), in the presence or absence of TYR (100 nM). ^aControl significantly different from E17G, ^bcontrol significantly different from E17G+TYR, ^cE17G significantly different from E17G+TYR. ($p < 0.05$). $n = 3-4$ animals per group

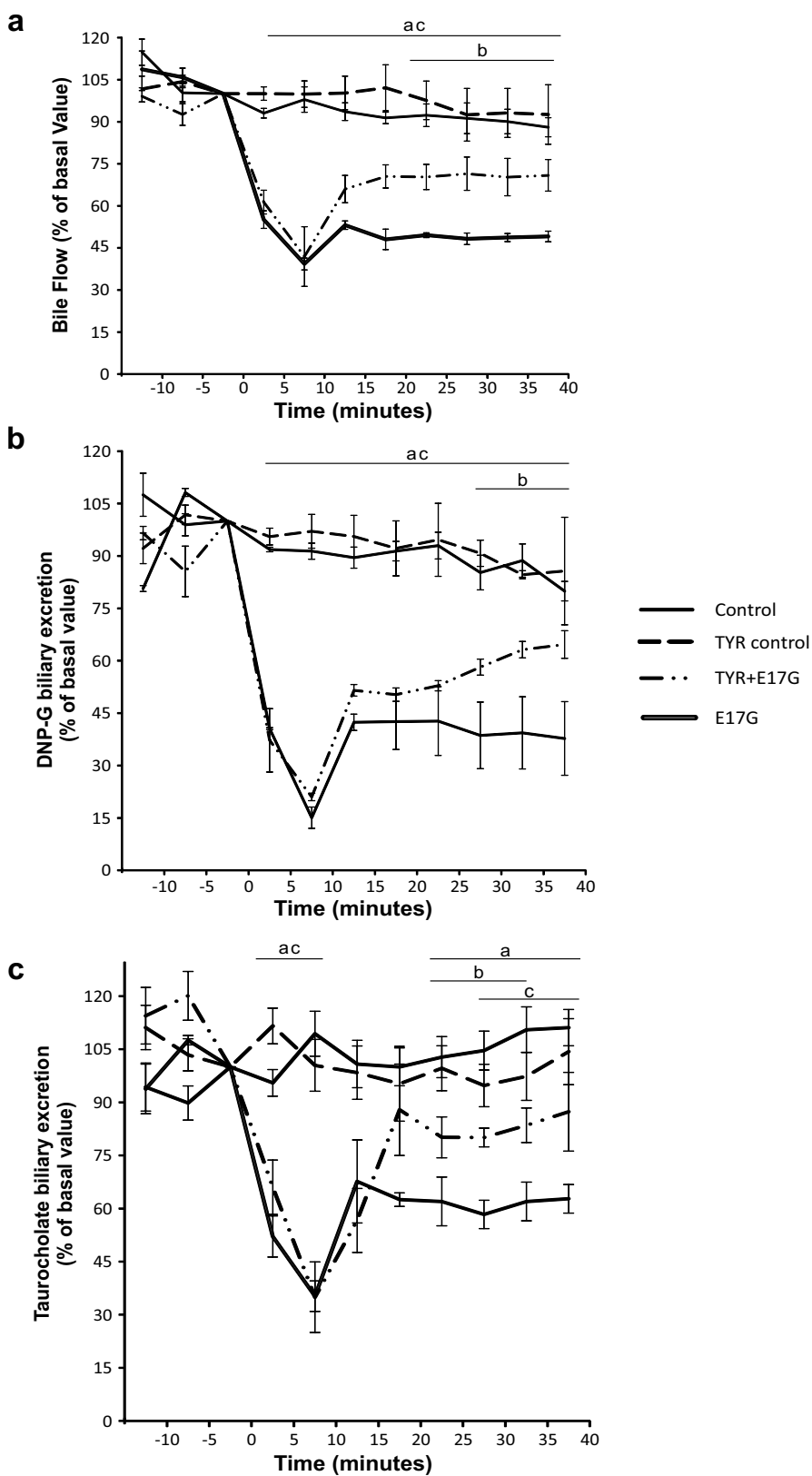


Fig. 9 IGF-1R inhibition prevents estradiol-17 β -D-glucuronide (E17G)-induced endocytic internalization of Abcb11 and Abcc2 in perfused rat liver. **a** Confocal images of E17G-induced internalization of Abcc2 and protection by tyrphostin AG1024 (TYR). Representative confocal images of immunostained liver samples displaying a containing of Abcc2 (green) and occludin (red). **b** Confocal images of E17G-induced internalization of Abcb11 and protection by tyrphostin AG1024 (TYR). Representative confocal images of immunostained liver samples displaying a containing of Abcb11 (green) and occludin (red). In control livers, both Abcc2 and Abcb11 were mainly confined to the canalicular space delineated by the tight junction-associated protein occludin. Following E17G (3 μ mol/liver), some canaliculi show intracellular fluorescence associated with Abcc2 or Abcb11 at a greater distance from the canalicular membrane (arrows), consistent with their delocalization. TYR (100 nM, 15 min previous to E17G) prevented the internalization of canalicular transporters, as illustrated by a control-like pattern of Abcc2 and Abcb11 distribution. TYR itself did not induce any changes in transporters localization. The densitometric analysis of the modification of the distribution of Abcc2 and Abcb11 by the different treatments is presented as additional Fig. 3 (color figure online)

participate the trafficking of the subunit $\beta\gamma$ at the endosomal level where it would interact with Rab11a (García-Regalado et al. 2008). Based on our results, in our model IGF-1R could participate in the trafficking of $\beta\gamma$ subunit to Rab11a-endosome. These Rab11a-endosomes are implicated in the microtubule-dependent recycling of canalicular transporters (Zucchetti et al. 2011) and according to our results this recycling would be blocked by IGR-IR and PI3K-Akt activation.

IGF-1R is expressed in hepatocyte but in low quantities (Qadir et al. 2015) and shares homology with another more abundant receptor, the insulin receptor. Hence, the effects ascribed to IGF-1R could potentially be the result of the activation of insulin receptor. Several pieces of evidence give support to a specific role of IGF-1R: first, siRNAs used in hepatocyte sandwich experiments were specific to IGF-1R and do not overlap with insulin receptor; second, TYR can inhibit insulin receptor but its IC50 is 5x the IC50 for IGR-IR (Párrizas et al. 1997) and greater than the concentration of TYR employed, finally, IGF-1, agonist of IGF-1R, reverted the protection of E17G-induced cholestasis by GPR30 inhibitor but insulin failed to do so even using a concentration 100 \times greater.

In conclusion, this study demonstrates the participation of IGF-1R in E17G-induced cholestasis. This receptor is activated by E17G and this activation is necessary to block the retrieval of the canalicular transporters Abcc2 and Abcb11. We also placed this protein in one of the three signaling pathways that leads to estrogen cholestasis described so far. E17G first activates GPR30 and then by other intermediate signaling proteins activates IGF-1R to lead through other intermediate signaling proteins to the activation of PI3K.

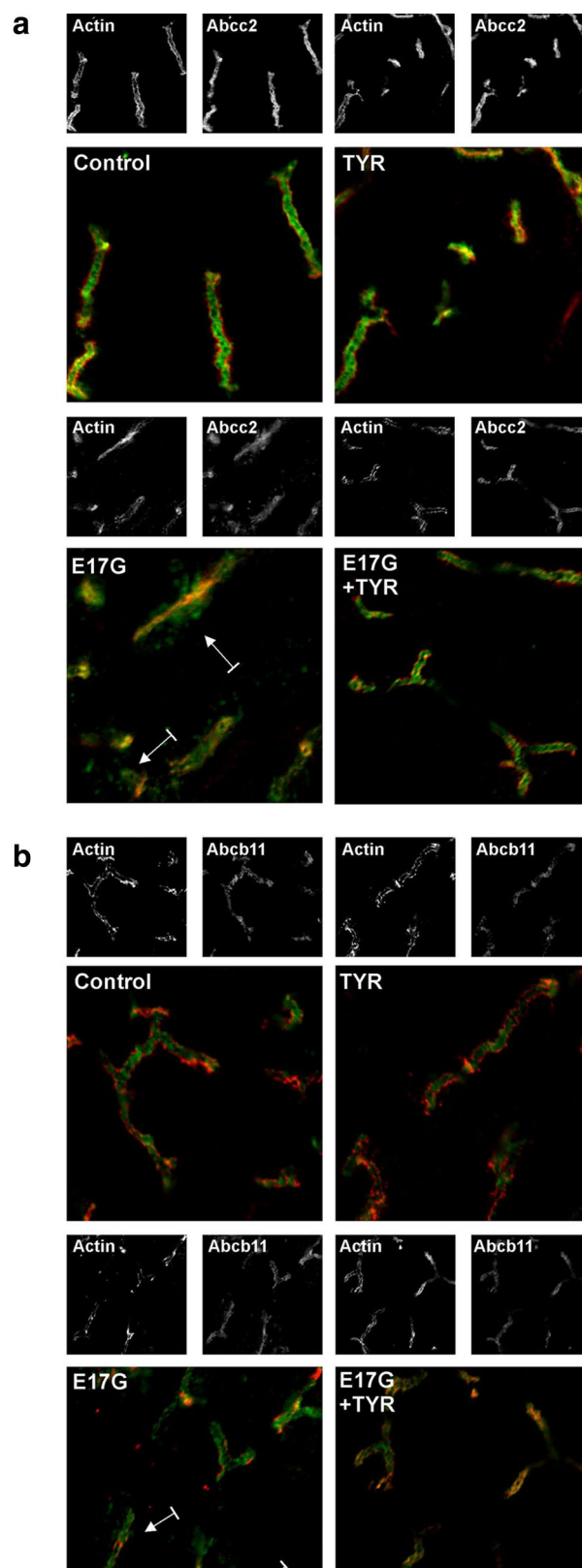
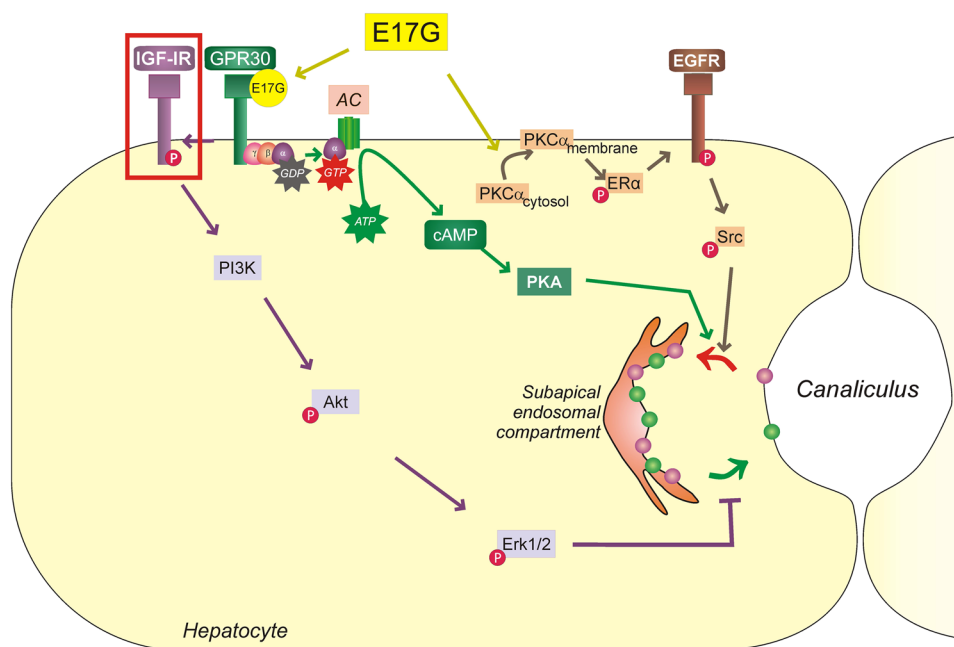


Fig. 10 Placement of IGF-1R among the signaling proteins that participate in E17G-induced cholestasis. According to the evidence gathered so far, E17G activates signaling proteins in three complementary pathways: two pathways initiate with the estrogen receptor GPR30 and in the other, the initial event detected is the translocation of PKC α from cytosol to the membrane. IGF-1R (box) is placed between GPR30 and PI3K, in a pathway whose activation delay the spontaneous reinsertion of the canalicular transporter-containing vesicles occurring during the recovery phase of the cholestasis



Acknowledgements We thank J. Pellegrino for assistance with confocal microscopy.

Compliance with ethical standards

Financial support This work was supported by grants from Agencia Nacional de Promoción Científica y Tecnológica (PICTs 2013 N° 1222 and 2013 N° 0974) and Consejo Nacional de Investigaciones Científicas y Técnicas (PIP 0217 and PUE IFISE 0089).

References

- Adlercreutz H, Tikkanen MJ, Wichmann K et al (1974) Recurrent jaundice in pregnancy. IV. Quantitative determination of urinary and biliary estrogens, including studies in pruritus gravidarum. *J Clin Endocrinol Metab* 38:51–57. doi:10.1210/jcem-38-1-51
- Barosso IR, Zucchetti AE, Boaglio AC et al (2012) Sequential activation of classic PKC and estrogen receptor α is involved in estradiol 17 β -D-glucuronide-induced cholestasis. *PLoS One* 7:e50711. doi:10.1371/journal.pone.0050711
- Barosso IR, Zucchetti AE, Miszczuk GS et al (2015) EGFR participates downstream of ER α in estradiol-17 β -D-glucuronide-induced impairment of Abcc2 function in isolated rat hepatocyte couplets. *Arch Toxicol* 90:891–903. doi:10.1007/s00204-015-1507-8
- Boaglio AC, Zucchetti AE, Sanchez Pozzi EJ et al (2010) Phosphoinositide 3-kinase/protein kinase B signaling pathway is involved in estradiol 17 β -D-glucuronide-induced cholestasis: complementarity with classical protein kinase C. *Hepatology* 52:1465–1476
- Boaglio AC, Zucchetti AE, Toledo FD et al (2012) ERK1/2 and p38 MAPKs are complementarily involved in estradiol 17 β -D-glucuronide-induced cholestasis: crosstalk with cPKC and PI3K. *PLoS One* 7:e49255. doi:10.1371/journal.pone.0049255
- Borst P, Elferink RO (2002) Mammalian ABC transporters in health and disease. *Annu Rev Biochem* 71:537–592. doi:10.1146/annurev.biochem.71.102301.093055
- Crocenzi FA, Mottino AD, Sánchez Pozzi EJ et al (2003a) Impaired localisation and transport function of canalicular Bsep in tauro-lithocholate induced cholestasis in the rat. *Gut* 52:1170–1177
- Crocenzi FA, Sanchez Pozzi EJ, Pellegrino JM et al (2003b) Preventive effect of silymarin against tauro-lithocholate-induced cholestasis in the rat. *Biochem Pharmacol* 66:355–364
- Crocenzi FA, Sanchez Pozzi EJ, Ruiz ML et al (2008) Ca²⁺-dependent protein kinase C isoforms are critical to estradiol 17 β -D-glucuronide-induced cholestasis in the rat. *Hepatology* 48:1885–1895
- Donner MG, Schumacher S, Warskulat U et al (2007) Obstructive cholestasis induces TNF-alpha- and IL-1-mediated periportal downregulation of Ntcp, Oatp1a4, and Oatp1b2. *Am J Physiol Gastrointest Liver Physiol* 293(6):G1134–G1146
- Esteller A (2008) Physiology of bile secretion. *World J Gastroenterol* 14:5641–5649
- Franco C, Bengtsson B-A, Johannsson G (2006) The GH/IGF-1 axis in obesity: physiological and pathological aspects. *Metab Syndr Relat Disord* 4:51–56. doi:10.1089/met.2006.4.51
- Garcia F, Kierbel A, Larocca MC et al (2001) The water channel aquaporin-8 is mainly intracellular in rat hepatocytes, and its plasma membrane insertion is stimulated by cyclic AMP. *J Biol Chem* 276:12147–12152
- García-Regalado A, Guzmán-Hernández ML, Ramírez-Rangel I et al (2008) G protein-coupled receptor-promoted trafficking of Gbeta1gamma2 leads to AKT activation at endosomes via a mechanism mediated by Gbeta1gamma2-Rab11a interaction. *Mol Biol Cell* 19:4188–4200. doi:10.1091/mbc.E07-10-1089
- Garcia-Segura LM, Arévalo M-A, Azcoitia I (2010) Interactions of estradiol and insulin-like growth factor-I signalling in the nervous system. In: *Progress in brain research*. pp 251–272
- Gatmaitan ZC, Arias IM (1995) ATP-dependent transport systems in the canalicular membrane of the hepatocyte. *Physiol Rev* 75:261–275
- Gautam A, Ng OC, Boyer JL (1987) Isolated rat hepatocyte couplets in short-term culture: structural characteristics and plasma membrane reorganization. *Hepatology* 7:216–223

- Kato H, Faria TN, Stannard B et al (1994) Essential role of tyrosine residues 1131, 1135, and 1136 of the insulin-like growth factor-I (IGF-I) receptor in IGF-I action. *Mol Endocrinol* 8:40–50. doi:10.1210/mend.8.1.7512194
- Kuemmerle JF, Murthy KS (2001) Coupling of the insulin-like growth factor-I receptor tyrosine kinase to Gi2 in human intestinal smooth muscle: G-dependent mitogen-activated protein kinase activation and growth. *J Biol Chem* 276:7187–7194. doi:10.1074/jbc.M011145200
- Lappano R, De Marco P, De Francesco EM et al (2013) Cross-talk between GPER and growth factor signaling. *J Steroid Biochem Mol Biol* 137:50–56. doi:10.1016/j.jsbmb.2013.03.005
- Maglova LM, Jackson AM, Meng XJ et al (1995) Transport characteristics of three fluorescent conjugated bile acid analogs in isolated rat hepatocytes and couplets. *Hepatology* 22:637–647
- Misra S, Varticovski L, Arias IM (2003) Mechanisms by which cAMP increases bile acid secretion in rat liver and canalicular membrane vesicles. *Am J Physiol Gastrointest Liver Physiol* 285(2):G316–G324
- Miszczuk GS, Barosso IR, Zucchetti AE et al (2015) Sandwich-cultured rat hepatocytes as an in vitro model to study canalicular transport alterations in cholestasis. *Arch Toxicol* 89:979–990. doi:10.1007/s00204-014-1283-x
- Miyata M (2004) Role of farnesoid X receptor in the enhancement of canalicular bile acid output and excretion of unconjugated bile acids: a mechanism for protection against cholic acid-induced liver toxicity. *J Pharmacol Exp Ther* 312:759–766. doi:10.1124/jpet.104.076158
- Mottino AD, Hoffman T, Jennes L et al (2001) Expression of multidrug resistance-associated protein 2 in small intestine from pregnant and postpartum rats. *Am J Physiol Gastrointest Liver Physiol* 280:G1261–G1273
- Mottino AD, Cao J, Veggi LM et al (2002) Altered localization and activity of canalicular Mrp2 in estradiol-17 β -D-glucuronide-induced cholestasis. *Hepatology* 35:1409–1419
- Mottino AD, Veggi LM, Wood M et al (2003) Biliary secretion of glutathione in estradiol 17beta-D-glucuronide-induced cholestasis. *J Pharmacol Exp Ther* 307:306–313
- Mottino AD, Crocenzi FA, Pozzi EJS et al (2005) Role of microtubules in estradiol-17beta-D-glucuronide-induced alteration of canalicular Mrp2 localization and activity. *Am J Physiol Gastrointest Liver Physiol* 288:G327–G336
- Párrizas M, Gazit A, Levitzki A et al (1997) Specific inhibition of insulin-like growth factor-I and insulin receptor tyrosine kinase activity and biological function by tyrphostins. *Endocrinology* 138:1427–1433. doi:10.1210/endo.138.4.5092
- Pfaffl MW, Horgan GW, Dempfle L (2002) Relative expression software tool (REST) for group-wise comparison and statistical analysis of relative expression results in real-time PCR. *Nucleic Acids Res* 30:e36
- Qadir XV, Chen W, Han C et al (2015) miR-223 Deficiency protects against Fas-induced hepatocyte apoptosis and liver injury through targeting insulin-like growth factor 1 receptor. *Am J Pathol* 185:3141–3151. doi:10.1016/j.ajpath.2015.08.020
- Roma MG, Milkiewicz P, Elias E, Coleman R (2000) Control by signaling modulators of the sorting of canalicular transporters in rat hepatocyte couplets: role of the cytoskeleton. *Hepatology* 32:1342–1356
- Song RX-D, Zhang Z, Chen Y et al (2007) Estrogen signaling via a linear pathway involving insulin-like growth factor I receptor, matrix metalloproteinases, and epidermal growth factor receptor to activate mitogen-activated protein kinase in MCF-7 breast cancer cells. *Endocrinology* 148:4091–4101. doi:10.1210/en.2007-0240
- Suleiman M, Singh R, Stewart C (2007) Apoptosis and the cardiac action of insulin-like growth factor I. *Pharmacol Ther* 114:278–294. doi:10.1016/j.pharmthera.2007.03.001
- Troncoso R, Ibarra C, Vicencio JM et al (2014) New insights into IGF-1 signaling in the heart. *Trends Endocrinol Metab* 25:128–137
- Vore M (1987) Estrogen cholestasis. Membranes, metabolites, or receptors? *Gastroenterology* 93:643–649
- Vore M, Liu Y, Huang L (1997) Cholestatic properties and hepatic transport of steroid glucuronides. *Drug Metabol Rev* 29:183–203
- Wang L, Soroka CJ, Boyer JL (2002) The role of bile salt export pump mutations in progressive familial intrahepatic cholestasis type II. *J Clin Invest* 110:965–972
- Wilton JC, Williams DE, Strain AJ et al (1991) Purification of hepatocyte couplets by centrifugal elutriation. *Hepatology* 14:180–183
- Yuan B, Latek R, Hossbach M et al (2004) siRNA Selection Server: an automated siRNA oligonucleotide prediction server. *Nucleic Acids Res* 32:W130–W134. doi:10.1093/nar/gkh366
- Zheng H, Worrall C, Shen H et al (2012) Selective recruitment of G protein-coupled receptor kinases (GRKs) controls signaling of the insulin-like growth factor I receptor. *Proc Natl Acad Sci USA* 109:7055–7060. doi:10.1073/pnas.1118359109
- Zucchetti AE, Barosso IR, Boaglio A et al (2011) Prevention of estradiol 17beta-D-glucuronide-induced canalicular transporter internalization by hormonal modulation of cAMP in rat hepatocytes. *Mol Biol Cell* 22:3902–3915. doi:10.1091/mbc.E11-01-0047
- Zucchetti AE, Barosso IR, Boaglio AC et al (2013) Hormonal modulation of hepatic cAMP prevents estradiol 17beta-D-glucuronide-induced cholestasis in perfused rat liver. *Dig Dis Sci* 58:1602–1614. doi:10.1007/s10620-013-2558-4
- Zucchetti AE, Barosso IR, Boaglio AC et al (2014) G-protein-coupled receptor 30/adenylyl cyclase/protein kinase A pathway is involved in estradiol 17{ β }-D-glucuronide-induced cholestasis. *Hepatology* 59:1016–1029. doi:10.1002/hep.26752